PERGAMON

International Journal of Solids and Structures 36 (1999) 35–64

INTERNATIONAL JOURNAL OF SOLIDS and STRUCTURES

A penny shaped crack in a transversely isotropic material under non-axisymmetric impact loads

Robert Rizza[a,*], Sudhakar Nair[b]

[a]*Department of Mechanical Engineering and Applied Mechanics, North Dakota State University, Fargo, North Dakota, U.S.A.*

[b]*Department of Mechanical, Materials and Aerospace Engineering, Illinois Institute of Technology, Chicago, Illinois, U.S.A.*

Received 23 November 1996; in revised form 5 September 1997

Abstract

A solution is given for problems involving non-axisymmetric dynamic impact loading of a penny shaped crack in a transversely isotropic medium. Laplace and Hankel transforms are used to reduce the equations of elasticity to integral equations, and solutions are obtained for the three modes of fracture. The stress intensity factors are determined for a penny shaped crack loaded by concentrated normal impact forces and concentrated radial shear impact forces. The integral equations are solved by numerical methods, and the results are plotted showing how the dynamic stress intensity factors are influenced by the asymmetric loading.
© 1998 Elsevier Science Ltd. All rights reserved.

1. Introduction

Many fibrous composites may be modeled as transversely isotropic materials with the stress field determined by five elastic constants (Christensen, 1979). The concept of the stress intensity factor (SIF) was shown to be applicable to such materials, since as in isotropic materials, the stress field at the crack tip was shown to have the square root singularities associated with cracks in isotropic solids, even though the stresses depended on the degree of anisotropy (Sih and Chen, 1981).

A penny shaped crack under general static loading in a transversely isotropic material has been investigated by numerous authors including Chen (1966) and Chen and Soni (1964). These static solutions have been collected in the text by Sih and Chen (1981) and Kassir and Sih (1977).

The basic outcome of these studies has been to show that the stress at the tip of the crack was dependent on the elastic constants of the solid. However, the stress intensity factor, for solids with infinite boundaries, was determined to be independent of the material constants and equal to the

*Corresponding author.

0020–7683/99/$—see front matter © 1998 Elsevier Science Ltd. All rights reserved
PII: S0020–7683(97)00274–6

value obtained for the isotropic case. If finite boundaries are imposed on the solid, or if more than one crack is located within the composite, then the stress intensity factor becomes dependent on the material constants.

Dynamic crack problems are not as readily solved as static ones, due to the complex behavior of the elastic waves near the crack faces. Known solutions may be divided into two groups.

The first of these two groups deals with harmonic or steady state loading. The arrival of a harmonic wave at the crack will produce a harmonic scattered wave. The total solution of the crack problem is the sum of the incident and scattered wave. Because the scattered wave carries information about the crack, only the scattered part of the solution determines the dynamic stress intensity factor.

Robertson (1966) studied the diffraction of harmonic waves on a penny shaped crack in an isotropic medium. The dynamic intensity factor for such a loading was determined by Mal (1968), for long wave lengths (low frequency), and found to be always larger than the static value. Radial and shear loading were discussed by Sih and Loeber (1969). These solutions which are for axisymmetric harmonic loading of the crack, are collected in the texts by Sih (1981) and Parton and Boriskovsky (1989).

Krenk and Schmidt (1982) have given a numerical solution of the diffraction problem by expansion of the displacement field in Fourier coefficients, an approach which will be used in this paper. Krenk and Schmidt did not determine expressions for the stress intensity factors. In 1983, Martin and Wickham, using an integral formulation derived by Martin, obtained the solution for the diffraction of harmonic waves for a penny shaped crack at an arbitrary angle of incidence. Martin and Wickham's solution is obtained in terms of Fourier expansions and coupled integral equations for the components of displacement. Furthermore, they obtained expressions for the dynamic stress intensity factors for general harmonic loading, although they gave no computational results.

Tsai (1988) determined the harmonic axisymmetric stress intensity factor for a penny shaped crack in a transversely isotropic material at low frequencies. Tsai used an integral equation approach and numerically obtained the harmonic SIF for two characteristic transversely isotropic materials: E-Glass Epoxy and Graphite Epoxy. He found very little difference in the values of the dynamic SIF for the two different transversely isotropic materials. In particular, Tsai obtained peak values of 1.59 times the static value for the E-Glass Epoxy and 1.58 times the static value for the Graphite Epoxy.

The second group involves transient response due to impact loading. Axisymmetric impact loading of a penny shaped crack in an isotropic material was first investigated by Embley and Sih (1971) for normal impact, and for torsional transient loading by Sih and Embley (1972). Both of these results along with others of interest in this area, are collected in the monograph by Sih (1977) and Parton and Boriskovsky (1989). For normal loading, Embley and Sih found that even for steel, with a Poisson's ratio of 0.29, the dynamic SIF had a maximum value of 1.23 times greater than the static value. Decreasing Poisson's ratio had the effect of decreasing the overshoot of the dynamic stress intensity factor. For impact loading of penny shaped cracks, as time becomes infinite, the dynamic stress intensity factor approaches the static value.

Solutions for axisymmetric dynamic loading of penny shaped cracks by concentrated forces in isotropic materials have been obtained by Chen et al. (1996). The authors used an integral equation approach to obtain a boundary integral for the problem under consideration. They show that the

location of the concentrated forces, which produces the largest value of the dynamic overshoot, differs from the location which produces the largest value of the static stress intensity factor.

Shindo and Nozaki (1987) determined the axisymmetric dynamic stress intensity factor for a penny shaped crack in a transversely isotropic material under impact loads. The paper examined both infinite and finite boundaries on the solid. The influence of different transversely isotropic materials on the dynamic SIF was found to be minimal. For the case of infinite boundaries, the dynamic SIF was determined to have a value of 1.45 times greater than the static value. The effect of the boundaries was to increase the value of the dynamic SIF.

In engineering materials more than one penny shaped crack may exist simultaneously. In order to solve problems involving multiple cracks, the stress field acting on any given crack must be obtained (Rizza, 1995). This stress field is determined from the sum of two contributions. The first contribution is due to the far-field applied loads. The second part is the resultant due to the influence of all other cracks located in the material. This second contribution includes terms which are asymmetric depending on the relative positions of the cracks. Therefore, in order to solve multiple crack problems, the solution for asymmetric loading of a penny shaped crack is desired. However, the solutions mentioned have considered only axisymmetric loadings.

The purpose of this work is to present a solution for the dynamic fracture of a penny shaped crack in a transversely isotropic under non-axisymmetric loads. The Laplace and Hankel transforms as well as the Fourier series will be used to reduce the equations of elastodynamics to integral equations. Numerically, for a typical transversely isotropic material, the stress intensity factors will be inverted to recover the time dependency for the title problem under concentrated normal and radial shear forces. Furthermore, these general solutions will be shown to reduce to known special cases.

1.1. *Formulation of the problem*

Consider a penny shaped crack located in an infinite transversely isotropic medium. Such a material may be used to model a fibrous composite with the z coordinate along the fiber direction. We assume the crack radius is of an order larger than the inhomogeneity of the material, so that the material may be considered homogeneous. A cylindrical coordinate system (r, θ, z) is used with the origin placed at the center of the crack and the crack occupying the region $0 \leqslant r \leqslant a, 0 \leqslant \theta \leqslant 2\pi$ and $z = 0$.

In the absence of body forces, the equations of motion are (Sokolnikof, 1987):

$$\frac{\partial \sigma_{rr}}{\partial r} + \frac{1}{r}\frac{\partial \sigma_{r\theta}}{\partial \theta} + \frac{\partial \sigma_{rz}}{\partial z} + \frac{\sigma_{rr} - \sigma_{\theta\theta}}{r} = \rho \frac{\partial^2 u}{\partial t^2} \tag{1a}$$

$$\frac{\partial \sigma_{r\theta}}{\partial r} + \frac{1}{r}\frac{\partial \sigma_{\theta\theta}}{\partial \theta} + \frac{\partial \sigma_{\theta z}}{\partial z} + \frac{2}{r}\sigma_{r\theta} = \rho \frac{\partial^2 v}{\partial t^2} \tag{1b}$$

$$\frac{\partial \sigma_{rz}}{\partial r} + \frac{1}{r}\frac{\partial \sigma_{\theta z}}{\partial \theta} + \frac{\partial \sigma_{zz}}{\partial z} + \frac{2}{r}\sigma_{rz} = \rho \frac{\partial^2 w}{\partial t^2} \tag{1c}$$

where u, v and w are the displacements in the radial, tangential and axial direction, respectively.

Furthermore, the components of stress are related to the strain through Hooke's law for transversely isotropic materials as:

$$\sigma_{rr} = C_{11}e_{rr} + C_{12}e_{\theta\theta} + C_{13}e_{zz} \tag{2a}$$

$$\sigma_{\theta\theta} = C_{12}e_{rr} + C_{11}e_{\theta\theta} + C_{13}e_{zz} \tag{2b}$$

$$\sigma_{zz} = C_{13}e_{rr} + C_{13}e_{\theta\theta} + C_{33}e_{zz} \tag{2c}$$

$$\sigma_{rz} = C_{44}e_{rz} \quad \sigma_{\theta z} = C_{44}e_{\theta z} \tag{2d}$$

$$\sigma_{r\theta} = \tfrac{1}{2}(C_{11} - C_{12})e_{r\theta} \tag{2e}$$

where the C's represent the elastic constants and e_{rr}, $e_{\theta\theta}$, e_{zz}, e_{rz}, $e_{\theta z}$, and $e_{r\theta}$ are the components of strain.

2. Formal solution

The equations of motion may be rewritten in terms of the displacement by substituting eqn set (2) into (1), and using the definitions of the strain components. Upon doing so, eqn (1) becomes

$$L_{11}(u) + L_{12}(v) + L_{13}(w) = L(u) \tag{3a}$$

$$L_{21}(u) + L_{22}(v) + L_{23}(w) = L(v) \tag{3b}$$

$$L_{31}(u) + L_{32}(v) + L_{33}(w) = L(w) \tag{3c}$$

The operators defined in eqn (3) are

$$L_{11}(f) = C_{11}\frac{\partial}{\partial r}\left[\frac{1}{r}\frac{\partial(rf)}{\partial r}\right] + C_{66}\frac{1}{r^2}\frac{\partial^2(f)}{\partial\theta^2} + C_{44}\frac{\partial^2(f)}{\partial z^2} \tag{4a}$$

$$L_{12}(f) = -(C_{11} + C_{66})\frac{1}{r^2}\frac{\partial(f)}{\partial\theta} + \frac{(C_{11} + C_{12})}{2}\frac{1}{r}\frac{\partial^2(f)}{\partial r\,\partial\theta} \tag{4b}$$

$$L_{13}(f) = (C_{13} + C_{44})\frac{\partial^2(f)}{\partial r\,\partial z} \tag{4c}$$

$$L_{21}(f) = (C_{11} + C_{66})\frac{1}{r^2}\frac{\partial(f)}{\partial\theta} \tag{4d}$$

$$L_{22}(f) = C_{66}\frac{\partial}{\partial r}\left[\frac{1}{r}\frac{\partial(rf)}{\partial r}\right] + C_{11}\frac{1}{r}\frac{\partial^2(f)}{\partial\theta^2} + C_{44}\frac{\partial^2(f)}{\partial z^2} \tag{4e}$$

$$L_{23}(f) = (C_{13} + C_{44})\frac{1}{r}\frac{\partial^2(f)}{\partial\theta\,\partial z} = L_{32} \tag{4f}$$

$$L_{31}(f) = (C_{13} + C_{44})\frac{\partial}{\partial z}\left[\frac{1}{r}\frac{\partial(rf)}{\partial r}\right] \tag{4g}$$

$$L_{33}(f) = C_{44}\frac{\partial}{r\,\partial r}\left[r\frac{\partial(f)}{\partial r}\right]+C_{33}\frac{\partial^2(f)}{\partial z^2}+C_{44}\frac{1}{r^2}\frac{\partial^2(f)}{\partial\theta^2} \tag{4h}$$

$$L(f) = \rho\frac{\partial^2(f)}{\partial t^2} \tag{4i}$$

with ρ being the density of the material.

Equation set (3) may be reduced by defining certain potential functions ϕ_i, $i = 1, 2, 3$ in the form

$$u = \frac{\partial}{\partial r}(\phi_1+\phi_2)+\frac{1}{r}\frac{\partial\phi_3}{\partial\theta} \tag{5a}$$

$$v = \frac{1}{r}\frac{\partial}{\partial\theta}(\phi_1+\phi_2)-\frac{\partial\phi_3}{\partial r} \tag{5b}$$

$$w = \frac{\partial}{\partial z}(m_1\phi_1+m_2\phi_2) \tag{5c}$$

The functions m_i, $r = 1, 2$ will be determined shortly.

Through the use of (5), the equations of motion take on the forms

$$C_{11}\left(\frac{\partial^2\chi}{\partial r^2}+\frac{1}{r}\frac{\partial\chi}{\partial r}\right)+\frac{C_{11}}{r^2}\frac{\partial^2\chi}{\partial\theta^2}+C_{44}\frac{\partial^2\chi}{\partial z^2}+(C_{13}+C_{44})\frac{\partial^2\psi}{\partial z^2} = \rho\frac{\partial^2\chi}{\partial t^2} \tag{6a}$$

$$\frac{C_{44}}{r}\frac{\partial}{\partial r}\left(r\frac{\partial\psi}{\partial r}\right)+\frac{(C_{13}+C_{44})}{r}\left(\frac{\partial}{\partial r}\left(r\frac{\partial\chi}{\partial r}\right)+\frac{\partial^2\chi}{r\,\partial\theta^2}\right)+\frac{C_{44}}{r^2}\frac{\partial^2\psi}{\partial\theta^2}+C_{33}\frac{\partial^2\psi}{\partial z^2} = \rho\frac{\partial^2\psi}{\partial t^2} \tag{6b}$$

$$C_{66}\frac{1}{r}\frac{\partial}{\partial r}\left(r\frac{\partial\phi_3}{\partial r}\right)+\frac{C_{66}}{r^2}\frac{\partial^2\phi_3}{\partial\theta^2}+C_{44}\frac{\partial^2\phi_3}{\partial z^2} = \rho\frac{\partial^2\phi_3}{\partial t^2} \tag{6c}$$

where $\chi = \phi_1+\phi_2$ and $\psi = m_1\phi_1+m_2\phi_2$. The problem has now been reduced to obtaining expressions for ϕ_1, ϕ_2, and ϕ_3.

In order to obtain these solutions, we assume the loading on the crack may be expanded in Fourier series, with respect to the polar angle θ, so that the potential functions may be taken in terms of sine and cosine functions. This reduces (6) to a set of equations which is two-dimensional.

Let us take $\phi_i = \bar{\phi}_i\exp(\mathrm{i}v\theta)$, $i = 1, 2, 3$, $v = 0, 1, \ldots$ and define $\bar{\chi} = \bar{\phi}_1+\bar{\phi}_2$, and $\bar{\psi} = m_1\bar{\phi}_1+m_2\bar{\phi}_2$ then equation set (6) becomes after some simplification

$$C_{11}\left(\frac{1}{r}\frac{\partial}{\partial r}\left(r\frac{\partial}{\partial r}\right)-\frac{v^2}{r^2}\right)\bar{\chi}+C_{44}\frac{\partial^2\bar{\chi}}{\partial z^2}+(C_{13}+C_{44})\frac{\partial^2\bar{\psi}}{\partial z^2} = \rho\frac{\partial^2\bar{\chi}}{\partial t^2} \tag{7a}$$

and

$$(C_{13}+C_{44})\left(\frac{1}{r}\frac{\partial}{\partial r}\left(r\frac{\partial}{\partial r}\right)-\frac{v^2}{r^2}\right)\bar{\chi}+C_{44}\left(\frac{1}{r}\frac{\partial}{\partial r}\left(r\frac{\partial}{\partial r}\right)\right)-\frac{v^2}{r^2}\bar{\psi}+C_{33}\frac{\partial^2\psi}{\partial z^2} = \rho\frac{\partial^2\bar{\psi}}{\partial t^2} \tag{7b}$$

$$C_{66}\left(\frac{1}{r}\frac{\partial}{\partial r}\left(r\frac{\partial}{\partial r}\right)-\frac{v^2}{r^2}\right)\bar{\phi}_3+C_{44}\frac{\partial^2\bar{\phi}_3}{\partial z^2}=\rho\frac{\partial^2\bar{\phi}_3}{\partial t^2} \tag{7c}$$

In eqn (7), the operator in the brackets may be reduced by the use of the Hankel transform of order v. The Laplace transform with transform variable p may be used to remove the dependency of eqn (1) on the time variable.

The Hankel transform of order v of a function $f(r)$ is defined by the integral expression (Andrews and Shivamoggi, 1988)

$$H_v\{f(r);r\to\xi\}=\int_0^\infty rf(r)J_v(\xi r)\,\mathrm{d}r \tag{8a}$$

where $J_v(\xi r)$ is the Bessel function of order v. The inverse of the Hankel transform is defined as

$$H_v^{-1}\{f(\xi);\xi\to r\}=\int_0^\infty \xi f(\xi)J_v(\xi r)\,\mathrm{d}\xi \tag{8b}$$

The Laplace integral transform of the function $F(p)$ with transform variable p of a function $f(t)$ is defined as the integral

$$F(p)=L\{f(t);t\to p\}=\int_0^\infty \exp(-pt)f(t)\,\mathrm{d}t \tag{9a}$$

and its inverse is given by

$$f(t)=L^{-1}\{F(p);p\to t\}=\frac{1}{2\pi i}\int_{Br}\exp(pt)F(p)\,\mathrm{d}p \tag{9b}$$

where Br indicates the Bromwich path of integration defined in the complex plane to the right of all singularities of $F(p)$.

Application of (8) and (9) to (7) shows that ϕ_1, ϕ_2, and ϕ_3 satisfy ordinary differential equations

$$(C_{44}+(C_{13}+C_{44})m_i)\frac{\partial^2\bar{\phi}_i}{\partial z^2}-\xi^2a_1\bar{\phi}_i=0 \tag{10a}$$

$$C_{33}m_i\frac{\partial^2\bar{\phi}_i}{\partial z^2}-\xi^2[(C_{13}+C_{44})+a_2]\bar{\phi}_i=0\quad i=1,2 \tag{10b}$$

$$C_{44}\frac{\partial^2\bar{\phi}_3}{\partial z}-\xi^2(C_{66}+\rho k^2)\bar{\phi}_3=0 \tag{10c}$$

where we have defined $k=p/\xi$ and $a_1=C_{11}+\rho k^2$, $a_2=C_{44}+\rho k^2$.

Equation (10) has a solution if we take

$$\frac{C_{44}+(C_{13}+C_{44})m_i(\xi,p)}{C_{11}+\rho k^2}=\frac{C_{33}m_i(\xi,p)}{(C_{13}+C_{44})+(C_{44}+\rho k^2)m_i(\xi,p)}=n_i(\xi,p)\quad i=1,2 \tag{11a}$$

$$n_3(\xi,p)=\frac{C_{44}}{C_{66}+\rho k^2} \tag{11b}$$

$$m_i(\xi,p)=\frac{a_1 n_i(\xi,p)}{C_{13}+C_{44}}=\frac{(C_{13}+C_{44})n_i(\xi,p)}{C_{33}-a_2 n_i(\xi,p)} \tag{11c}$$

The constants n_i, $i=1,2$ are the solutions of the quadratic equation

$$a_1a_2n^2+n((C_{13}+C_{44})^2-C_{33}a_1-C_{44}a_2)+C_{33}C_{44}=0 \tag{12}$$

In the case where the dynamic terms vanish (that is, $p=0$), we see that (11) and (12) reduce to that of the static case (Sih and Chen, 1981). Let M_1, M_2, N_1, N_2, and N_3 be constants which are the solutions of eqn (12), when $p=0$, that is, the static solution. Then N_1 and N_2 satisfy the quadratic equation

$$C_{11}C_{44}N^2+N((C_{13}+C_{44})^2-C_{33}C_{11}-C_{44}^2)+C_{33}C_{44}=0 \tag{13}$$

and (11) becomes

$$\frac{C_{44}+(C_{13}+C_{44})M_i}{C_{11}}=\frac{C_{33}M_i}{(C_{13}+C_{44})+C_{44}M_i}=N_i \quad i=1,2 \tag{14a}$$

$$N_3=\frac{C_{44}}{C_{66}} \tag{14b}$$

$$M_i=\frac{C_{11}N_i}{C_{13}+C_{44}}=\frac{(C_{13}+C_{44})N_i}{C_{33}-C_{44}N_i} \tag{14c}$$

Now suppose that the loading is dynamic but that the material is isotropic. Then by putting $C_{44}=C_{66}=\mu$, $C_{66}=(C_1-C_{12})/2$, $C_{13}=C_{12}=\lambda$ and $C_{11}=\lambda+2\mu$, the dynamic isotropic solution is obtained. In this case, λ and μ are the Lamé constants. Equation (11) becomes

$$n_i=\frac{\xi^2}{\gamma_i^2} \quad i=1,2 \quad \text{and} \quad n_3=n_1 \quad \text{(isotropic and dynamic)} \tag{15a}$$

where

$$\gamma_i^2=\left(\xi^2+\frac{p^2}{c_i^2}\right) \tag{15b}$$

and the constants c_1 and c_2 are the well-known wave speeds for an isotropic material. In particular, $c_1^2=[(\lambda+2G)/\rho]$ is the dilatational wave speed and $c_2^2=(\mu/\rho)$ is the transverse or shear wave speed (Sokolnikoff, 1987).

The functions $m_i(\xi,p)$ reduce to

$$m_1=1, \quad m_2=\frac{\xi^2}{\gamma_2^2} \quad \text{(isotropic and dynamic)} \tag{16}$$

The differential equations in (10) have exponential solutions of the form $\phi\sim\exp(\pm\alpha_i\xi z)$. We assume that $\alpha_i=(1/n_i)^{1/2}$ have positive real parts for $z>0$. Furthermore, we can assume without

any loss of generality that the applied stresses σ_{zz}, σ_{rz}, are even functions and $\sigma_{\theta z}$ is an odd function, as will be the case for most applied loads under consideration. Then, by using the solutions of (10), the inverse Hankel transform of $\bar{\phi}_i$, the potentials may be written in the form

$$\phi_i(\xi,p) = \sum_{v=0}^{\infty} \{H_v^{-1}[B_i^v(\xi,p)\exp(-\alpha_i\xi z);\ \xi \to r]\}\cos v\theta \quad i=1,2 \tag{17a}$$

$$\phi_3(\xi,p) = \sum_{v=1}^{\infty} \{H_v^{-1}[B_3(\xi,p)\exp(-\alpha_3\xi z);\ \xi \to r]\}\sin v\theta \tag{17b}$$

If the eveness and oddness of the applied stresses are changed then the sine and cosine terms in eqn (17) are interchanged. The functions $B_i^v(\xi,p)$, $i=1,2,3$ are to be determined from the boundary conditions.

For the sake of simplicity, let us define

$$d_i^v(\xi,p) = B_i^v(\xi,p)\exp(-\alpha_i\xi z) \quad i=1,2,3 \tag{18a}$$

$$h_j^v(\xi,p) = [(1+m_j(\xi,p))C_{44}+\rho k^2 m_j(\xi,p)] \quad j=1,2 \tag{18b}$$

$$f_1^v(\xi,p) = \xi^2[\alpha_1(1+m_1(\xi,p))d_1^v(\xi,p)+\alpha_2(1+m_2(\xi,p))d_2^v(\xi,p)+\alpha_3 d_3^v(\xi,p)] \tag{18c}$$

$$f_2^v(\xi,p) = \xi^2[\alpha_1(1+m_1(\xi,p))d_1^v+\alpha_2(1+m_2(\xi,p))d_2^v(\xi,p)-\alpha_3 d_3^v(\xi,p)] \tag{18d}$$

Then, in the Laplace transform domain, the displacements become

$$u^* = \frac{1}{2}\sum_{v=0}^{\infty}\cos v\theta\{H_{v-1}^{-1}[\xi(d_1^v(\xi)+d_2^v(\xi))]+H_{v+1}^{-1}[\xi(d_3^v(\xi)-d_1^v(\xi)-d_2^v(\xi))]\} \tag{19a}$$

$$v^* = -\frac{1}{2}\sum_{v=1}^{\infty}\sin v\theta\{H_{v-1}^{-1}[\xi(d_1^v(\xi)+d_2^v(\xi)+d_3^v(\xi))]H_{v+1}^{-1}[\xi(d_1^v(\xi)+d_2^v(\xi)-d_3^v(\xi))]\} \tag{19b}$$

$$w^* = -\sum_{v=0}^{\infty}\cos v\theta\{H_v^{-1}[\xi(\alpha_1 m_1 d_1^v(\xi)+\alpha_2 m_2 d_2^v(\xi))]\} \tag{19c}$$

Likewise, the stresses may be written in the form

$$\sigma_{rz}^* = -\frac{C_{44}}{2}\sum_{v=0}^{\infty}\cos v\theta\{H_{v-1}^{-1}[f_1^v(\xi,p)]-H_{v+1}^{-1}[f_2^v(\xi,p)]\} \tag{20a}$$

$$\sigma_{\theta z}^* = \frac{C_{44}}{2}\sum_{v=1}^{\infty}\sin v\theta\{H_{v-1}^{-1}\{H_{v-1}^{-1}[f_1^v(\xi,p)]+H_{v+1}^{-1}[f_2^v(\xi,p)]\} \tag{20b}$$

$$\sigma_{zz}^* = \sum_{v=0}^{\infty}\cos v\theta\{H_v^{-1}[\xi^2[h_1^v(\xi,p)d_1^v(\xi,p)+h_2^v(\xi,p)d_2^v(\xi,p)]] \tag{20c}$$

Boundary conditions for specific loading cases are now employed to determine the values of $B_i^v(\xi)$. The general loading may be split into two parts: the symmetric part and the skew-symmetric part. We consider each of these problems separately.

3. Solution of the symmetric part

Let the symmetric loading on the crack for $z = 0$ be a transient in time such as an impact load of $\sigma(r, \theta)$ applied at time $t = 0$. The boundary conditions on the crack may be written in the form

$$\sigma_{zz} = -\sigma(r, \theta)H(t) \quad 0 \leqslant r \leqslant a \tag{21a}$$

$$\sigma_{rz} = \sigma_{\theta z} = 0 \quad r > a \tag{21b}$$

$$w = 0 \quad r > a \tag{21c}$$

where $H(t)$ is the Heaviside step function used to model the time dependency. The Laplace transform with transform variable p may be applied to the boundary conditions. Then, the normal load on the crack may be expanded in Fourier cosine (or sine) series (Chen, 1966) with Fourier coefficients $a_v(r)$ given by

$$a_0(r) = \frac{1}{\pi}\int_0^{\pi} -\frac{\sigma(r, \theta)}{p}\,\mathrm{d}\theta \tag{22a}$$

and

$$a_v(r) = \frac{2}{\pi}\int_0^{\pi} -\frac{\sigma(r, \theta)}{p}\cos v\theta\,\mathrm{d}\theta \quad v = 1, 2, \ldots \tag{22b}$$

The boundary conditions require that the shear stresses be zero for $r > 0$. Using eqns (20a) and (20b) along with (21b), for any arbitrary value of v, it is found that $B_3^v(\xi) = 0$ and that

$$B_2^v(\xi, p) = -\sqrt{\frac{n_2(\xi)}{n_1(\xi)}}\,\frac{(1+m_1(\xi))}{1+m_2(\xi))}\,B_1^v(\xi, p) \tag{23}$$

Applying this expression to (20c) and (19c), we obtain the dual integral equation for $v = 0, 1, 2 \ldots$ and $z = 0$:

$$\int_0^{\infty} \xi G(\xi, p)\phi^v(\xi)J_v(\xi r)\,\mathrm{d}\xi = a_v^*(r, p) \quad 0 \leqslant r < a \tag{24a}$$

$$\int_0^{\infty} \phi^v(\xi, p)J_v(\xi r)\,\mathrm{d}\xi = 0 \quad r > a \tag{24b}$$

where $a_v^* = a_v/\eta$. The constant η is the value of $G(\xi)$ when $\xi \to \infty$ (or $p = 0$), that is, when the static limit is reached. Thus, when the applied loads are static, eqn (24) reduces to the form given by Sih and Chen (1981) or Chen (1966).

When the material is isotropic, eqn (24) reduces to that obtained by Sih (1977) for axisymmetric loading of the penny shaped crack. In this case, put $v = 0$, apply the reductions given in (15) and (16) and redefine $A(\xi, p) = \phi^0(\xi, p)/\xi$. Then, the function $G(\xi, p)$ becomes

$$G(\xi, p) = g_1(\xi, p) = \frac{c_2^2}{2p\gamma_1\mu\xi}\left[\left(2\xi^2 + \left(\frac{2}{c_2}\right)^2 - 4\gamma_1\gamma_2\xi^2\right)\right] \quad \text{(isotropic and dynamic)} \tag{25}$$

which is the form obtained by Sih (1977). Martin and Wickham (1983) have obtained solutions for harmonic loading of the penny shaped crack in an isotropic material. Our solutions reduce to those of Martin and Wickham, by replacing ρp^2 with $-\rho w^2$, since solutions for harmonic loadings in the time domain are similar for impact loadings in the Laplace transfer plane.

The functions $\phi^v(\xi, p)$, $G(\xi)$ and η are defined as

$$\phi^v(\xi,p) = \sqrt{n_1(\xi)}\,\frac{(1+m_2(\xi))}{(m_1(\xi)-m_2(\xi))}\,B_1^v(\xi,p) \tag{26a}$$

$$G(\xi) = \frac{[\sqrt{n_1(\xi)}(1+m_2(\xi))h_1(\xi)-\sqrt{n_2(\xi)}(1+m_1(\xi))h_2(\xi)]}{(m_1(\xi)-m_2(\xi))} \tag{26b}$$

$$\eta = \frac{C_{44}(1+M_1)(1+M_2)[\sqrt{N_1}-\sqrt{N_2}]}{(M_1-M_2)} \tag{26c}$$

The dual integral eqn (24) is a special form of the equation considered by Sneddon (1966). It may be solved by following Sih and Chen (1981) if we take

$$\phi^v(\xi) = \xi^{1/2}\int_0^a f^v(t,p)J_{v+(1/2)}(\xi t)\,\mathrm{d}t \tag{27}$$

where $f^v(t,p)$ is the solution of the Fredholm integral equation

$$f^v(t,p)+\int_0^a f^v(\zeta,p)K_1^v(\zeta,t)\,\mathrm{d}\zeta = \frac{t^{(1/2)-v}}{\eta}\sqrt{\frac{2}{\pi}}\int_0^t \frac{r^{1+v}a_v(r,p)\,\mathrm{d}r}{\sqrt{t^2-r^2}} \tag{28}$$

and the kernel $K(\zeta, t)$ is given by the integral expression

$$K_1^v(\zeta,t) = t\int_0^\infty \xi\left[\frac{G(\xi)}{\eta}-1\right]J_{v+(1/2)}(\xi t)J_{v+(1/2)}(\xi\zeta)\,\mathrm{d}\xi \tag{29}$$

Since $G(\xi)\to\eta$ as $\xi\to\infty$, the integral given in (29) is convergent. When $p = 0$, that is, for the static case, the kernel $K(\zeta, t)$ vanishes since $G(\xi)/\eta = 1$ when $p = 0$. Thus, for static applied loads, eqn (28) reduces to the form given by Sih and Chen (1981) or Chen (1966).

If the material is isotropic, then (28) reduces to the form obtained by Sih and Chen (1977) with $G(\xi, p)$ replaced by $g_1(\xi, p)$ as given in expression (25).

4. Symmetric stress intensity factor

With the symmetric part reduced to the solution of an integral equation, an expression for the opening mode (K_I) stress intensity factor may now be determined. If we take (16c), expand by integrating by parts, substitute (19) with $z = 0$ and use the definition for the opening mode stress intensity factor (Sih and Chen, 1981), we obtain in the Laplace transform plane

$$K_{\mathrm{I}}^{*}(p) = -\frac{2\eta}{\pi a}\sum_{v=0}^{\infty} f^{v}(a,p)\cos v\theta \tag{30}$$

The stress intensity factor in the time domain is given by the inversion of (30).

5. Solution of the skew-symmetric part

The second half of the general dynamic loading is the skew-symmetric loading which may be described by suddenly applied shear stresses on the crack faces. If shear loads are applied at time $t = 0$, appropriate boundary conditions may be taken for $z = 0$ and $0 \leqslant \theta \leqslant 2\pi$ in the form

$$\sigma_{rz} = -\tau_1(r,\theta)H(t) \quad 0 \leqslant r \leqslant a \tag{31a}$$

$$\sigma_{\theta z} = \tau_2(r,\theta)H(t) \quad 0 \leqslant r \leqslant a \tag{31b}$$

$$\sigma_{zz} = 0 \quad r > 0 \tag{31c}$$

$$u = v = 0 \quad r > a \tag{31d}$$

where τ_1 and τ_2 are given functions.

Application of the Laplace transform may be used to reduce eqn (31).

Furthermore, we may expand in Fourier series with coefficients $c_v(r)$ and $d_v(r)$ given by

$$c_0 = \frac{1}{\pi}\int_0^{\pi}\frac{\tau_1}{p}(r,\theta)\,\mathrm{d}\theta \tag{32a}$$

$$c_v = -\frac{2}{\pi}\int_0^{\pi}\frac{\tau_1}{p}(r,\theta)\cos v\theta\,\mathrm{d}\theta \quad v = 1,2,\ldots \tag{32b}$$

$$d_v = \frac{2}{\pi}\int_0^{\pi}\frac{\tau_2}{p}(r,\theta)\sin v\theta\,\mathrm{d}\theta \quad v = 1,2,\ldots \tag{32c}$$

Applying eqn (20c) to (31c), the normal stress condition requires

$$B_2^{v}(\xi,p) = -\frac{((1+m_1(\xi,p))C_{44}+\rho k^2 m_1(\xi,p))}{((1+m_2(\xi,p))C_{44}+\rho k^2 m_2(\xi,p))}B_1^{v}(\xi,p) \tag{33}$$

Substitution of (33) into (20a), (20b), (19a) and (19b), and use of the boundary conditions (31a), (31b) and (31d) results in the simultaneous dual integral equation

$$\int_0^{\infty}\xi(\Gamma_1(\xi)B_1^{v}(\xi,p)+\alpha_3 B_3^{v}(\xi,p))J_{v-1}(\xi r)\,\mathrm{d}\xi = \frac{C_v+D_v}{2} \quad 0 \leqslant r < a \tag{34a}$$

$$\int_0^{\infty}\xi(\Gamma_1(\xi)B_1^{v}(\xi,p)-\alpha_3 B_3^{v}(\xi,p))J_{v+1}(\xi r)\,\mathrm{d}\xi = \frac{D_v-C_v}{2} \quad 0 \leqslant r < a \tag{34b}$$

$$\int_0^\infty \xi(\Gamma_2(\xi)B_1^v(\xi,p)+B_3^v(\xi,p))J_{v-1}(\xi r)\,\mathrm{d}\xi = 0 \quad r > a \tag{34c}$$

$$\int_0^\infty \xi(\Gamma_2(\xi)B_1^v(\xi,p)-B_3^v(\xi,p))J_{v+1}(\xi r)\,\mathrm{d}\xi = 0 \quad r > a \tag{34d}$$

where $C_v(r) = 2c_v(r)/C_{44}$ and $D_v(r) = 2d_v(r)/C_{44}$ and

$$\Gamma_1(\xi) = \sqrt{\frac{1}{n_1(\xi)}}\left[(1+m_1(\xi))-\sqrt{\frac{n_1(\xi)}{n_2(\xi)}}\frac{((1+m_1(\xi))C_{44}+\rho k^2 m_1(\xi))}{((1+m_2(\xi))C_{44}+\rho k^2 m_2(\xi))}(1+m_2(\xi))\right] \tag{35a}$$

$$\Gamma_2(\xi) = 1-\frac{((1+m_1(\xi))C_{44}+\rho k^2 m_1(\xi))}{((1+m_2(\xi))C_{44}+\rho k^2 m_2(\xi))} \tag{35b}$$

When $v = 0$, that is, for the case of pure radial shear and no torsion, the equations uncouple and simplify so that $B_3^v(\xi) = 0$.

If we set

$$B_1^v(\xi,p) = -2\phi(\xi,p), \quad \frac{\Gamma_1(\xi,p)}{\Gamma_2(\xi,p)} = \frac{C_{44}}{a_2}\alpha_1\alpha_2 G(\xi,p),$$

then $\phi(\xi,p)$ is given as

$$\phi(\xi) = \xi^{1/2}\int_0^a g^v(t,p)J_{3/2}(\xi t)\,\mathrm{d}t \tag{36}$$

where $g^v(t,p)$ is the solution of the Fredholm integral equation

$$g^v(t,p)+\int_0^a g^v(\zeta,p)K_2^v(\zeta,t)\,\mathrm{d}\zeta = \frac{1}{2G^*}\sqrt{\frac{2}{\pi t}}\int_0^t \frac{r^2 C_0(r,p)\,\mathrm{d}r}{\sqrt{t^2-r^2}} \tag{37}$$

and where the kernel $K_2^v(\zeta,t)$ is given as

$$K_2^v(\zeta,t) = t\int_0^\infty \xi\left[\alpha_1\alpha_2\frac{C_{44}G(\xi,p)}{a_2 G^*}-1\right]J_{3/2}(\xi t)J_{3/2}(\xi\zeta)\,\mathrm{d}\xi \tag{38}$$

The constant G^* is obtained when $\xi \to \infty$ and has a value given by

$$G^* = \lim_{\substack{\xi\to\infty \\ p\to 0}}\frac{\Gamma_1}{\Gamma_2} = \frac{\eta}{C_{44}\sqrt{N_1 N_2}} \tag{39}$$

Because $(\Gamma_1(\xi)/\Gamma_2(\xi))/G^* \to 1$ as $\xi \to \infty$, the kernel is bounded at the upper limit. Furthermore, in the static limit, that is, when $p = 0$, $K_2^v(\zeta,t) = 0$, since $(\Gamma_1(\xi)/\Gamma_2(\xi))/G^* = 1$. Then, eqn (37) reduces to that obtained by Sih and Chen (1981) for the static counterpart of the loading under consideration.

If the material is isotropic, then we have

$$\alpha_1\alpha_2\frac{C_{44}G(\xi,p)}{a_2G^*}=\frac{\gamma_1}{\gamma_2}g_1(\xi,p)\quad\text{(isotropic and dynamic)}\tag{40}$$

which is the form given in Sih (1977).

When $v\geqslant 1$, the solution of (34) is much more involved. The solution follows if we define $\mu=v-1, f_1^v(\xi,p)=G^*\Gamma_2(\xi)B_1(\xi,p)$ and $f_2^v(\xi,p)=AB_3(\xi,p)$, and then subtract from both sides of (34a), the expression

$$\int_0^\infty \xi\left(\left(\frac{\gamma(\xi)}{G}-1\right)f_1^v(\xi,p)+\left(\frac{\alpha_3(\xi)}{A}-1\right)f_2^v(\xi,p)\right)J_\mu(\xi r)\,\mathrm{d}\xi\tag{41}$$

and from (34b), the expression

$$\int_0^\infty \xi\left(\left(\frac{\gamma(\xi)}{G}-1\right)f_1^v(\xi,p)+\left(1-\frac{\alpha_3(\xi)}{A}\right)f_2^v(\xi,p)\right)J_{\mu+2}(\xi r)\,\mathrm{d}\xi\tag{42}$$

equation set (34) is reduced to a form of the simultaneous dual integral equations considered by Westmann (1965)

$$\int_0^\infty \xi(f_1^v(\xi,p)+f_2^v(\xi,p))J_\mu(\xi r)\,\mathrm{d}\xi=h_1^*(r,p)\quad 0\leqslant r<a\tag{43a}$$

$$\int_0^\infty \xi(-f_1^v(\xi,p)+f_2^v(\xi,p))J_{\mu+2}(\xi r)\,\mathrm{d}\xi=h_2^*(r,p)\quad 0\leqslant r<a\tag{43b}$$

$$\int_0^\infty (N^*f_1^v(\xi,p)+f_2^v(\xi,p))J_\mu(\xi r)\,\mathrm{d}\xi=0\quad r>a\tag{43c}$$

$$\int_0^\infty (-N^*f_1^v(\xi,p)+f_2^v(\xi,p))J_{\mu+2}(\xi r)\,\mathrm{d}\xi=0\quad r>a\tag{43d}$$

where N^* and A are constants defined as

$$N^*=\frac{\sqrt{N_3}(M_2-M_1)}{(1+M_1)(1+M_2)(\sqrt{N_1}-\sqrt{N_2})}\tag{44a}$$

$$A=\lim_{\xi\to\infty}\alpha_3(\xi)=\sqrt{N_3}=\sqrt{\frac{C_{44}}{C_{66}}}\tag{44b}$$

and the right hand side of (43) is given by

$$h_1^*(r,p)=h_1(r,p)-\int_0^\infty \xi(g_{11}(\xi)f_1^v(\xi,p)+g_{12}f_2^v(\xi,p))J_\mu(\xi r)\,\mathrm{d}\xi\tag{45a}$$

$$h_2^*(r,p) = h_2(r,p) - \int_0^\infty \xi(g_{21}(\xi) f_1^\nu(\xi,p) + g_{22}(\xi) f_2^\nu(\xi,p)) J_{\mu+2}(\xi r)\,\mathrm{d}\xi \tag{45b}$$

with

$$g_{11}(\xi) = \left(\alpha_1\alpha_2 C_{44}\frac{G(\xi)}{a_2 G^*} - 1\right) = g_{21}(\xi) \tag{46a}$$

$$g_{12}(\xi) = \left(\frac{\alpha_3(\xi)}{A} - 1\right) = -g_{22}(\xi) \tag{46b}$$

When $p = 0$, that is, for the static case, $g_{11} = g_{12} = g_{21} = g_{22} = 0$ and $h_1^*(r,p) = h_1(r)$ and $h_2^*(r,p) = h_1(r)$. Thus, equation set (43) reduces to the equations given in Sih and Chen (1981) and Chen (1966) for the general skew-symmetric loading of the static counterpart.

If the material under consideration is isotropic and the loading is dynamic, then the quantities g_{ij} do not vanish, but take on the forms

$$g_{11}(\xi) = \left(\frac{\gamma_1}{\gamma_2} g_1(\xi,p) - 1\right) = g_{21}(\xi) \quad \text{(isotropic and dynamic)} \tag{47a}$$

$$g_{12}(\xi) = \left(\frac{\gamma_2}{A\xi} - 1\right) = -g_{22}(\xi) \quad \text{(isotropic and dynamic)} \tag{47b}$$

The simultaneous dual integral equations may now be solved by using Westmann's approach. The solution follows, if we take

$$f_1^\nu(\xi,p) = \xi^{1/2}\int_0^a [\phi_1^\nu(t,p) J_{\mu+(1/2)}(\xi t) + \phi_2^\nu(t,p) J_{\mu+(5/2)}(\xi t)]\,\mathrm{d}t \tag{48a}$$

$$f_2^\nu(\xi,p) = \xi^{1/2}\int_0^a [N^*\phi_1^\nu(t,p) J_{\mu+(1/2)}(\xi t) - \phi_2^\nu(t,p) J_{\mu+(5/2)}(\xi t)]\,\mathrm{d}t \tag{48b}$$

with

$$\phi_1^\nu(t,p) = \sqrt{\frac{2}{\pi}}\,\frac{t^{-[\mu-(1/2)]}}{(1+N^*)}\int_0^t \frac{r^{\mu+1} h_1^*(r,p)\,\mathrm{d}r}{\sqrt{t^2-r^2}} \tag{49a}$$

$$\phi_2^\nu(t,p) = (1-N^*)\left\{\frac{\phi_1^\nu(t,p)}{2} - \left(\mu+\frac{3}{2}\right)t^{-[\mu+(3/2)]}\int_0^t \phi_1^\nu(\tau,p)\tau^{-[\mu+(3/2)]}\,\mathrm{d}\tau\right\} - \frac{t^{-[\mu+(3/2)]}}{\sqrt{2\pi}}\int_0^t \frac{r^{\mu+3} h_2^*(r,p)\,\mathrm{d}r}{\sqrt{t^2-r^2}} \tag{49b}$$

The expressions for $\phi_1^\nu(t,p)$ and $\phi_2^\nu(t,p)$ can be further simplified for numerical work by substituting for h_1^* and h_2^*, that is, eqn (45). After some lengthy manipulations, and substituting $\mu = \nu - 1$, we obtain integral equations of Fredholm type for $\phi_1^\nu(t,p)$ and $\phi_2^\nu(t,p)$.

These integral equations are

$$\phi_1^v(t,p)+\int_0^a (K_{11}(\zeta,t)\phi_1^v(\zeta,p)+K_{12}(\zeta,t)\phi_2^v(\zeta,p))\,\mathrm{d}\zeta = \sqrt{\frac{2}{\pi}}\,\frac{t^{-[v-(3/2)]}}{(1+N^*)}\int_0^t \frac{r^v h_1(r,p)\,\mathrm{d}r}{\sqrt{t^2-r^2}} \tag{50a}$$

and

$$\phi_2^v(t,p)+\int_0^a (K_{21}(\zeta,t)\phi_1^v(\zeta,p)+K_{22}(\zeta,t)\phi_2^v(\zeta,p))\,\mathrm{d}\zeta$$

$$= \sqrt{\frac{2}{\pi}}\,\frac{(1-N^*)}{(1+N^*)t^v}\left\{\frac{t^{(3/2)}}{2}\int_o^t \frac{r^v h_1(r,p)\,\mathrm{d}r}{\sqrt{t^2-r^2}} - \frac{\left(v+\frac{1}{2}\right)}{\sqrt{t}}\int_0^t r^v h_1(r,p)\sqrt{t^2-r^2}\,\mathrm{d}r\right\}$$

$$+\frac{t^{-[v+(1/2)]}}{\sqrt{2\pi}}\int_0^t \frac{r^{v+2}h_2(r,p)\,\mathrm{d}r}{\sqrt{t^2-r^2}} \tag{50b}$$

where

$$K_{11}(\zeta,t) = \frac{t}{(1+N^*)}\int_0^\infty \xi\{g_{11}(\xi)+N^*g_{12}(\xi)\}J_{v-(1/2)}(\xi\zeta)J_{v-(1/2)}(\xi t)\,\mathrm{d}\xi \tag{51a}$$

$$K_{12}(\zeta,t) = \frac{t}{(1+N^*)}\int_0^\infty \xi\{g_{11}(\xi)-g_{12}(\xi)\}J_{v+(3/2)}(\xi\zeta)J_{v+(1/2)}(\xi t)\,\mathrm{d}\xi \tag{51b}$$

$$K_{21}(\zeta,t) = \frac{t}{2}\int_0^\infty \xi(g_{21}(\xi)+N^*g_{22}(\xi))J_{v-(1/2)}(\xi\zeta)J_{v+(3/2)}(\xi t)\,\mathrm{d}\xi\}$$

$$-\left(\frac{1-N^*}{1+N^*}\right)\left(v+\frac{1}{2}\right)\int_0^\infty (g_{11}(\xi)+N^*g_{12}(\xi))J_{v-(1/2)}(\xi\zeta)J_{v+(1/2)}(\xi t)\,\mathrm{d}\xi + \frac{1-N^*}{2}K_{11}(\zeta,t) \tag{51c}$$

$$K_{22}(\zeta,t) = \frac{t}{2}\int_0^\infty \xi(g_{21}(\xi)-g_{22}(\xi))J_{v+(3/2)}(\xi\zeta)J_{v+(3/2)}(\xi t)\,\mathrm{d}\xi$$

$$-\left(\frac{1-N^*}{1+N^*}\right)\left(v+\frac{1}{2}\right)\int_0^\infty (g_{11}(\xi)-g_{12}(\xi))J_{v+(3/2)}(\xi\zeta)J_{v+(1/2)}(\xi t)\,\mathrm{d}\xi + \frac{1-N^*}{2}K_{12}(\zeta,t) \tag{51d}$$

In the case of static loading, that is, when $p = 0$, eqns (50) and (51) reduce to those given in Sih and Chen (1981) for the general skew-symmetric static loading since $K_{ij}(\zeta,t) = 0$, $i,j = 1,2$ when $p = 0$.

For an isotropic material under dynamic loading, the equations have the same form as given by (50) however, the functions $g_{ij}(\xi,p)$, $i,j = 1,2$ are replaced with the forms as given in (47). If the loading is due to torsion, the sine term is interchanged with the cosine term and vice versa in equations (20), then $B_1^v(x,p) = B_2^v(x,p) = 0$, $v = 0,1,2,\ldots$ and $B_3^0(x,p)$ satisfies the integral equa-

tion obtained by Sih and Embley (1972) for the torsion of a penny shaped crack by impact loads in an isotropic material. Thus, the solution for general loading reduces to the known special case of twisting of a penny shaped crack by dynamic loads.

6. Skew-symmetric stress intensity factors

With the solution to the skew-symmetric dynamic loading of the penny shaped crack given by eqns (37) for $v = 0$ and (48a) and (48b) for $v \geqslant 1$, the corresponding sliding (K_{II}) and tearing mode (K_{III}) stress intensity factors may be determined.

The stress intensity factors are obtained by expanding (20a) and (20b) using integration by parts and then using the definitions for K_{II} and K_{III} (Sih and Chen, 1981).

The stress intensity factors in the Laplace transform plane are obtained to have the forms

$$K_{II}(p) = \frac{C_{44}}{a\sqrt{2\pi}}\left\{-g(a,p)G^* + 2\sum_{v=0}^{\infty}[\phi_1^v(a,p) - \phi_2^v(a,p)]\cos v\theta\right\} \tag{52a}$$

$$K_{III}(p) = -\frac{C_{44}}{a}\sqrt{\frac{2}{\pi}}\sum_{v=1}^{\infty}[N^*\phi_1^v(a,p) + \phi_2^v(a,p)]\sin v\theta \tag{52b}$$

The corresponding stress intensity factors in the time domain are given by the Laplace inversion of these equations.

It is important to note that if the evenness and oddness of the loading are changed, eqns (50) are still valid provided that the sine term is interchanged with the cosine term and vice versa. This is the case for pure torsion and no radial shear.

7. Numerical examples

In general, dynamic loads on a penny shaped crack may be arbitrary in time, as well as vary along the faces of the crack. By superposing the solution for a Heaviside type load, solutions for loads which are arbitrary in time can be constructed (Freund, 1986; or Rizza, 1995).

E-Glass Epoxy will be used in the examples which follow. The material constants characterizing this material (in 10^4 MPa) are: $C_{11} = 1.493$, $C_{12} = 0.6567$, $C_{13} = 0.5244$, $C_{33} = 4.727$, $C_{44} = 0.4745$ (Tsai, 1988). The various parameters can be non-dimensionalized by defining $T = tC_2/a$, $\zeta = as$, $x = a\xi$, $P = pa/C_2$, $\rho = r/a$ and $\tau = t/a$.

The integrals will be evaluated numerically. The improper integrals are first mapped from the domain $\xi \in [0, \infty]$ to $x \in [0, 1]$, then the IMSL routine QDAG is used with a 30–61 point globally adaptive Gauss–Kronrod rule (Piesens et al., 1983). Such rules are designed for highly oscillatory integrands.

Example 1: *Axisymmetric dynamic impact loads*

The solution for dynamic axisymmetric loading of the penny shaped crack found in the Shindo and Nozaki (1987) can be obtained from (28) and (30) through proper choice of the Fourier coefficients.

For axisymmetric dynamic loading, the boundary condition (17a) takes the form

$$\sigma_{zz} = -\sigma H(t) \quad 0 \leqslant r \leqslant a \tag{53}$$

where σ is a constant stress impacting over the crack faces at time $t = 0$. After taking the Laplace transform of (20) the only nonzero Fourier coefficient given by eqn (22) is $a_0 = \sigma/p$. Furthermore, the severity of the crack is defined by the SIF as given by eqn (30). Since all but the first term in the Fourier series expansion are zero, the stress intensity factor becomes

$$K_1^* = \sqrt{\frac{2}{\pi}}\,\sigma\sqrt{a}F^0(a,p) \tag{54}$$

where

$$F^0(\tau,P) = -\frac{P\eta\tau}{\sigma}\sqrt{\frac{\pi\tau}{2}}f^0(\tau,P)$$

is the solution of (28) for $v = 0$.

Thus, we have

$$F^0(a\tau,P) + \frac{2}{\pi}\int_0^1 \tau s F^0(as,P)K_1^0(as,a\tau)\,\mathrm{d}s = 1 \tag{55}$$

with the kernel given by

$$K_1^0(as,a\tau) = \int_0^\infty \left(\frac{G(ax)}{\eta} - 1\right)\sin(x\tau)\sin(xs)\,\mathrm{d}s \tag{56}$$

where we have used $J_{1/2}(z) = \sqrt{(2/\pi z)}\sin(z)$.

The improper integral in (56) was solved using the IMSL routine QDAWF. The integral eqn (55) was solved using the method of Nystrom (Press et al., 1985) wherein, the integral over s is expanded in Gauss–Legendre quadrature points and weights.

The value of the corresponding static stress intensity factor is obtained from eqn (30). The function $f^0(a,0)$ may be obtained from static counterpart of eqn (28), that is, when $p = 0$. Then, the integral over $[0,a]$ in eqn (28) vanishes, because $K_1^0(\zeta,t) = 0$ since $G(\xi)/\eta = 1$ when $p = 0$. Equation (28) becomes

$$f^0(t,0) = -\frac{\sigma}{\eta}\sqrt{\frac{2t}{\pi}}\int_0^t \frac{r\,\mathrm{d}r}{\sqrt{t^2-r^2}} \tag{57}$$

The integral on the right hand side of (57) is of elementary form. Upon integration (57) becomes

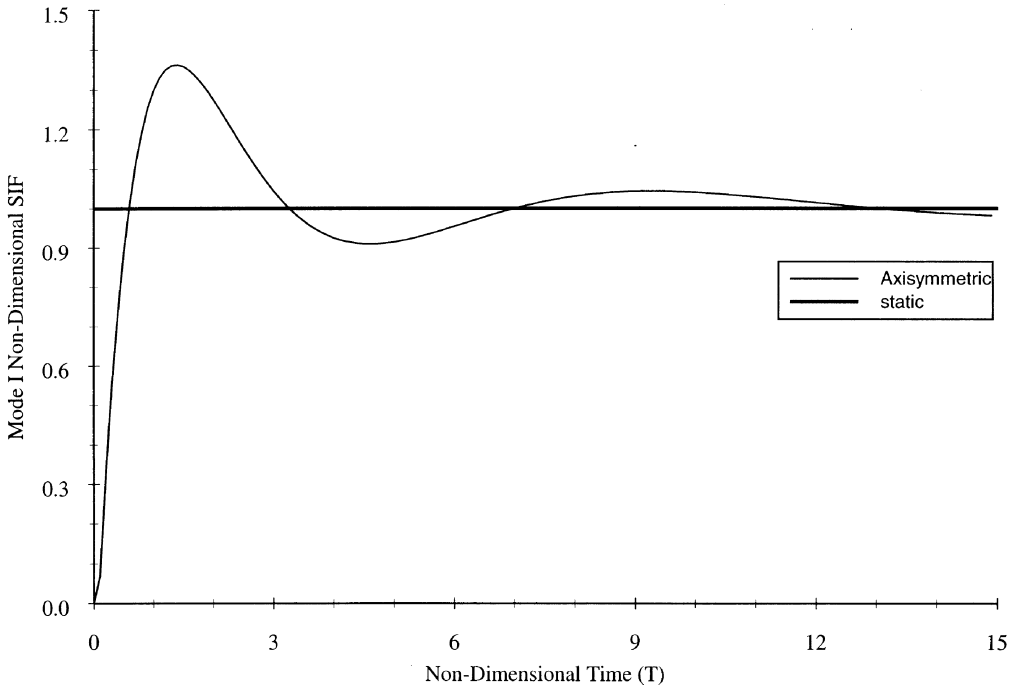

Fig. 1. Variation of Mode I non-dimensional SIF with T for axisymmetric loading.

$$f^0(t,0) = -\frac{\sigma t^{3/2}}{\sqrt{2\pi\eta}} \tag{58}$$

Now by substituting (58) with $t = a$ into (30), along with $v = 0$, the corresponding static stress intensity factor is obtained

$$K_{IS} = \sqrt{\frac{2}{\pi}}\,\sigma\sqrt{a} \tag{59}$$

Notice that this is the well-known static SIF for a uniform axisymmetric loading of the penny shaped crack (Kassir and Sih, 1975).

Equation (54) can be divided by (59) to give a non-dimensional SIF. This stress intensity factor can be obtained for all values of time by using the method of Papoulis (Miller and Guy, 1966) to carry out the Laplace inversion through numerical means.

The value of the axisymmetric opening mode dynamic SIF non-dimensionalized with respect to K_{IS} is plotted in Fig. 1. The results in Fig. 1 may be compared to similar results obtained by Shindo and Nozaki (1987). We obtain a maximum value of the non-dimensional SIF factor of 1.36 times the static value at a non-dimensional time value of $T = 1.5$. This is in agreement with the results obtained by Shindo and Nozaki.

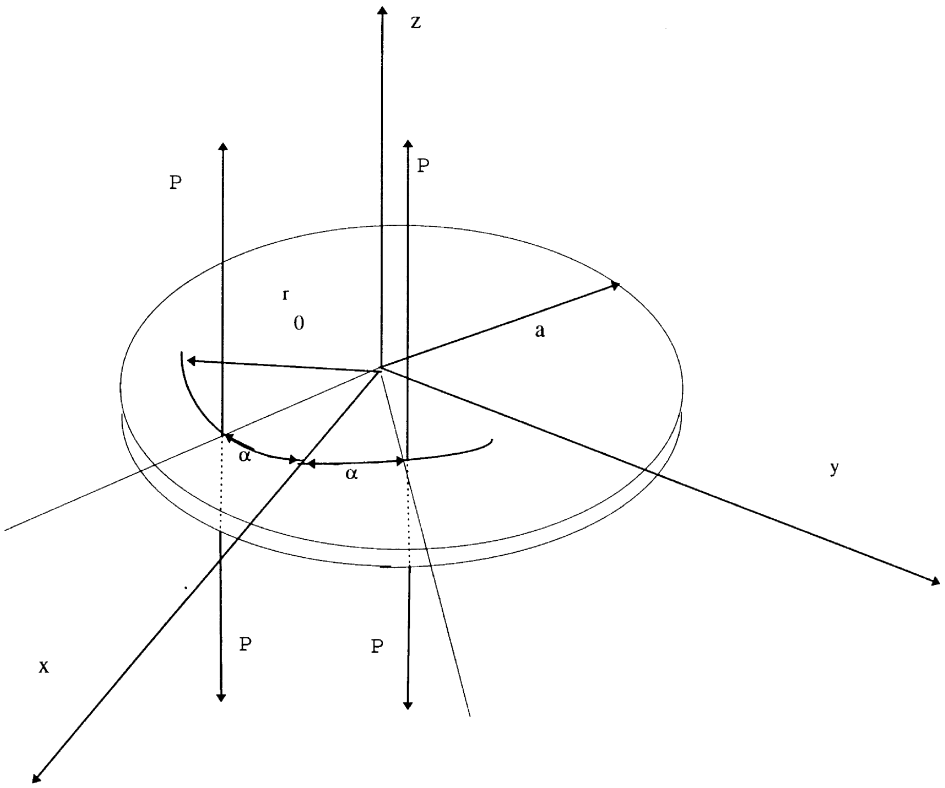

Fig. 2. Penny shaped crack with concentrated normal loads P.

Example 2: *Concentrated normal forces*

Consider a penny shaped crack loaded by two concentrated loads of magnitude P applied at the upper and lower crack surfaces at the points $r = r_0$; $\theta = \pm\alpha$ by a unit step load at $t = 0$ (Fig. 2).

For the loading under consideration, the Fourier coefficients may be obtained by taking the applied load in the form

$$\sigma(t) = -\frac{P}{r}\delta(r-r_0)\delta(\theta \pm \alpha) \tag{60}$$

then, the Fourier coefficients are obtained by substitution of (60) into (22).

The Fourier coefficients take on the forms

$$a_0 = \frac{1}{\pi}\int_0^{\pi} -\frac{P}{r}\delta(r-r_0)\delta(\theta \pm \alpha)\,\mathrm{d}\theta$$

$$= -\frac{P}{r}\delta(r-r_0) \tag{61a}$$

$$a_v = \frac{2}{\pi}\int_0^{\pi} -\frac{P}{r}\delta(r-r_0)\delta(\theta \pm \alpha)\cos v\theta \, \mathrm{d}\theta$$

$$= -\frac{2P}{\pi r}\delta(r-r_0)\cos v\theta \quad v = 1, 2, \ldots \tag{61b}$$

Substitution of (61) into the right hand side of (28) and by the use of the non-dimensional parameters defined previously along with the definition

$$f^v(\tau, P) = C_v F^v(\tau, P) H(\tau-\rho_0)\tau^{1/2} \tag{62}$$

reduces eqn (20) to

$$F^v(\tau, P) + \frac{2}{\pi}\int_{\rho_0}^{1} \tau s F^v(s, P) K_1^v(s, \tau)\, \mathrm{d}s = \frac{1}{\tau^{v+1}\sqrt{1-\left(\frac{\rho_0}{\tau}\right)}} \tag{63}$$

where

$$K_1^v(s, \tau) = \int_0^{\infty} x^2 \left[\frac{G(ax)}{\eta} - 1\right] j_v(x\tau) j_v(xs)\, \mathrm{d}x \tag{64}$$

in terms of $j_v(y)$ the spherical Bessel function of y which is defined as

$$j_n(y) = \left(\frac{\pi}{2z}\right)^{1/2} J_{n+1/2}(y) \tag{65}$$

In the Laplace transform plane, the dynamic stress intensity factor, $K_{\mathrm{I}}(P)$, may be non-dimensionalized by dividing by the corresponding value for a similar crack loaded by static forces, K_{IS} (Sih and Chen, 1981). The non-dimensional form of the dynamics SIF is obtained by inversion, that is,

$$\frac{K_{\mathrm{I}}(T)}{K_{\mathrm{IS}}} = \frac{\sqrt{1-\rho_0^2}}{2\pi i}\int_{Br}\left[\frac{F^0(1, P) + 2\sum_{v=1}^{\infty}\rho_0^v F^v(1, P)\cos v\alpha \cos v\theta}{1 + 2\sum_{v=1}^{\infty}\rho_0^v \cos v\alpha \cos v\theta}\right]\frac{\exp(PT)\,\mathrm{d}P}{P} \tag{66}$$

where *Br* indicates the Bromwich path of integration.

In the case where $\rho_0 = 0$, the right hand side of (63) is singular. In order to remove this singularity, we take eqn (63) and define

$$g^0(a\tau, p) = F^0(a\tau, P) - \frac{1}{\tau^{v+1}} \tag{67}$$

Substitution of (67) into (63) along with $v = 0$ gives

$$g^0(a\tau, P)+\frac{2}{\pi}\int_0^1 \tau s K_1^0(as, a\tau)g^0(a\zeta, P)\,\mathrm{d}\zeta = -\frac{2}{\pi}\int_0^1 \tau K_1^0(as, a\tau)\,\mathrm{d}\zeta \tag{68}$$

The right hand side of (68) is no longer singular. Furthermore, it may be reduced from a double to a single integral by substitution of $K_1^0(as, at)$ and interchanging the order of integration, that is,

$$\begin{aligned} -\frac{2}{\pi}\int_0^1 \tau K_1^0(as, a\tau)\,\mathrm{d}\zeta &= -\frac{2}{\pi}\tau\int_0^\infty \left\{\left(\frac{G(ax)}{\eta}-1\right)\sin x\tau\left(\int_0^1 \frac{\sin xs}{s}\,\mathrm{d}s\right)\right\}\mathrm{d}x \\ &= -\frac{2}{\pi}\tau\int_0^\infty \left\{Si(x)\left(\frac{G(ax)}{\eta}-1\right)\sin x\tau\right\}\mathrm{d}x \end{aligned} \tag{69}$$

where $Si(x)$ is the sine integral of x (Andrews, 1985).

The integral equation becomes

$$g^0(a\tau, P)+\frac{2}{\pi}\int_0^1 \tau s g^0(a\zeta, P)K_1^0(as, a\tau)\,\mathrm{d}\zeta = -\frac{2\tau}{\pi}\int_0^\infty Si(x)\left(\frac{G(ax)}{\eta}-1\right)\sin x\tau\,\mathrm{d}x \tag{70}$$

and $K_1^0(as, at)$ is given by eqn (56).

The inversion required by eqn (66) was achieved by using the numerical method of Papoulis (Miller and Guy, 1966). Equations (63) and (70) were solved using the method of Nystrom (Press et al., 1985). It was found that the series expansions in (63) and (70) could be truncated after four terms, which gave an absolute error between the third and fourth term of less than 1.0×10^{-4}.

The variation of the non-dimensional dynamic stress intensity factor with non-dimensional time is plotted in Figs 3–7. In particular, Fig. 3 shows the case when $\rho_0 = 0.0$, $\alpha = 0^\circ$. As can be seen from the figure, the dynamic stress intensity factor increases with time until it overshoots the static value. The maximum value of the overshoot is 32% larger than the static value. This maximum value occurs at $T = 2.2$. As time progresses, the value of the dynamic stress intensity factor approaches the static value.

From Fig. 4, with $\rho_0 = 0.25$, $\alpha = 0^\circ$, the maximum value of the dynamic overshoot is obtained at $\theta = \pi/2$ and $T = 1.3$, where the magnitude achieves a value of 1.36 times the static. For $\theta = 0$, the overshoot has a maximum value of 22% larger than the static SIF and occurs at $T = 1.1$. Furthermore, the time that it takes for the overshoot to occur increases as the angular position from the load increases, so that for $\theta = 180^\circ$, the overshoot occurs at $T = 1.4$.

If the load is moved to $\rho_0 = 0.5$, $\alpha = 0^\circ$, then the amount of overshoot decreases as can be seen by comparing Fig. 4 and Fig. 3. As the applied loads are moved even farther from the center of the crack to the position $\rho_0 = 0.75$, $\alpha = 0^\circ$, the overshoot of the dynamic stress intensity factor continues to decrease. The maximum value for the overshoot still occurs at $\theta = 90^\circ$, where it achieves a value of 1.25 times the static value at $T = 1.1$. The values of the overshoot have decreased to 5% larger than the static value at $T = 1.1$ for $\theta = 90^\circ$ and 1.14 times the static value at $T = 1.2$ for $\theta = 180^\circ$.

Thus, by comparing Figs 4–6, for any given value of θ, the magnitude of the dynamic overshoot decreases as ρ_0 increases. This is because the integral in eqn (63) is due to the complex combinations between the Laplace transform variable and the material constants. As the radial position increases,

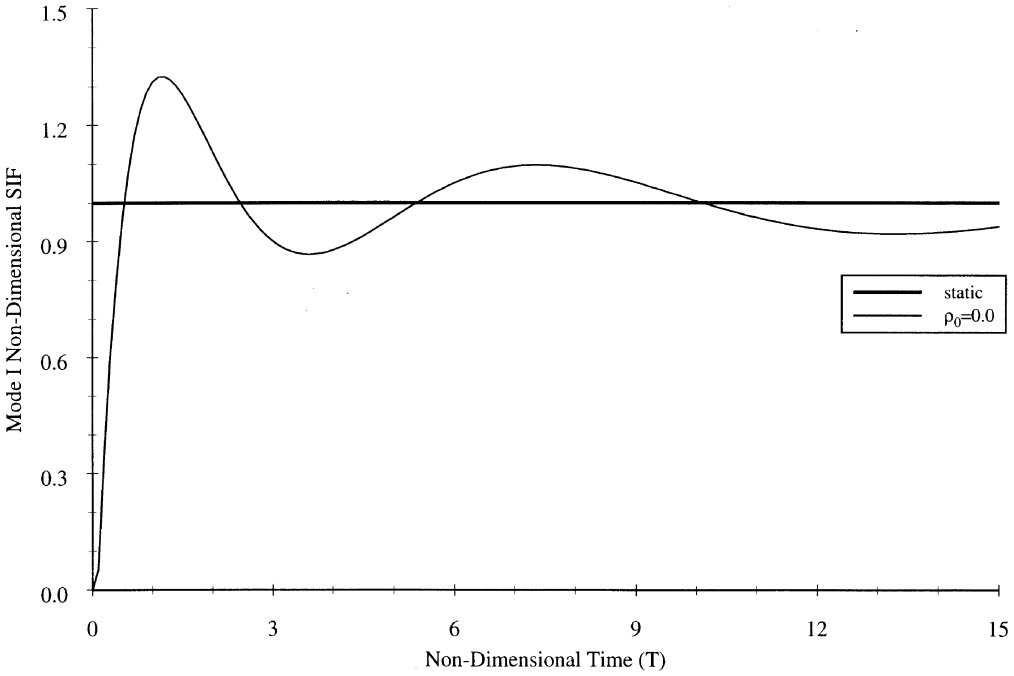

Fig. 3. Non-dimensional SIF for normal applied loads at $\rho_0 = 0.0$, $\alpha = 0^\circ$.

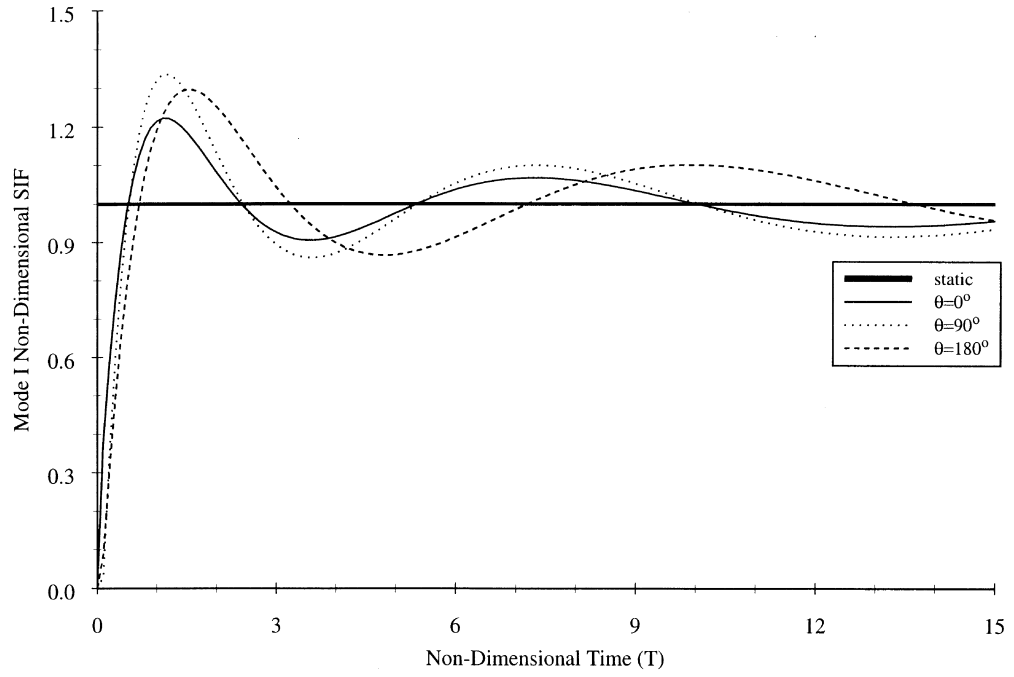

Fig. 4. Non-dimensional SIF for normal applied loads at $\rho_0 = 0.25$, $\alpha = 0^\circ$.

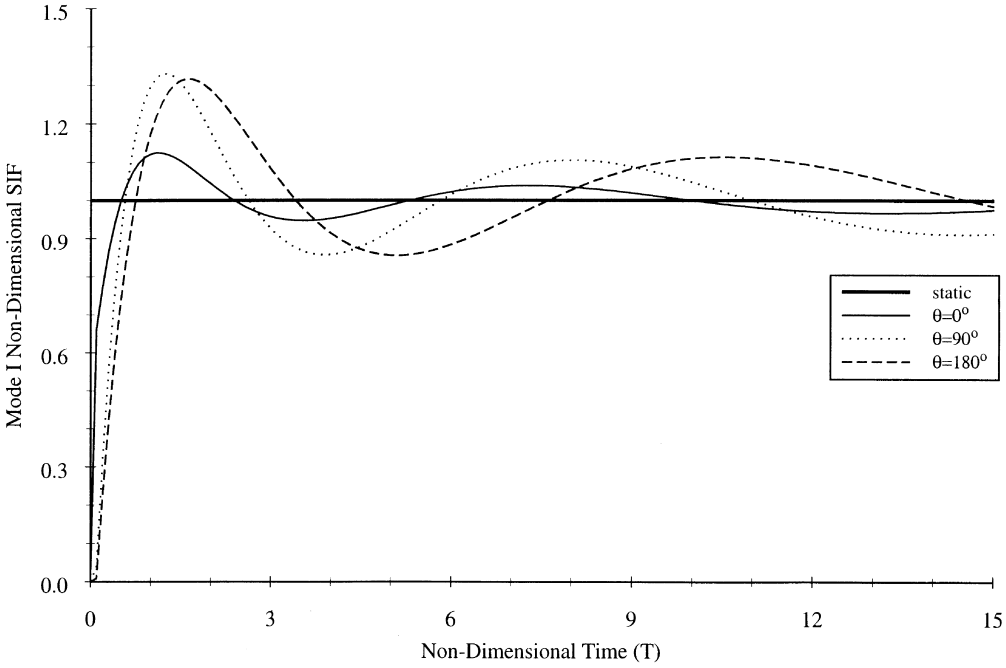

Fig. 5. Non-dimensional SIF for normal applied loads at $\rho_0 = 0.50$, $\alpha = 0^\circ$.

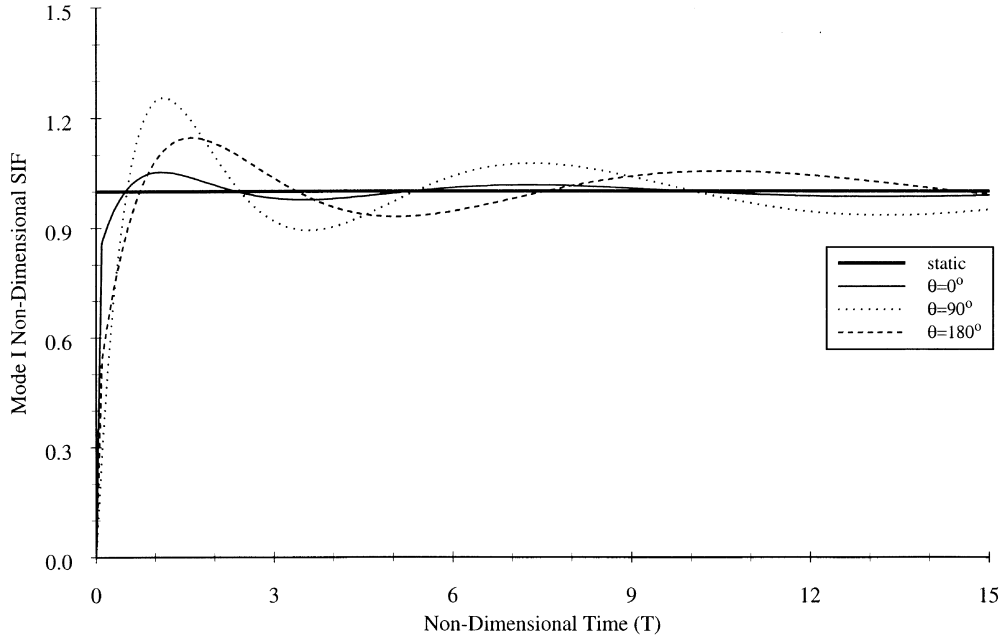

Fig. 6. Non-dimensional SIF for normal applied loads at $\rho_0 = 0.75$, $\alpha = 0^\circ$.

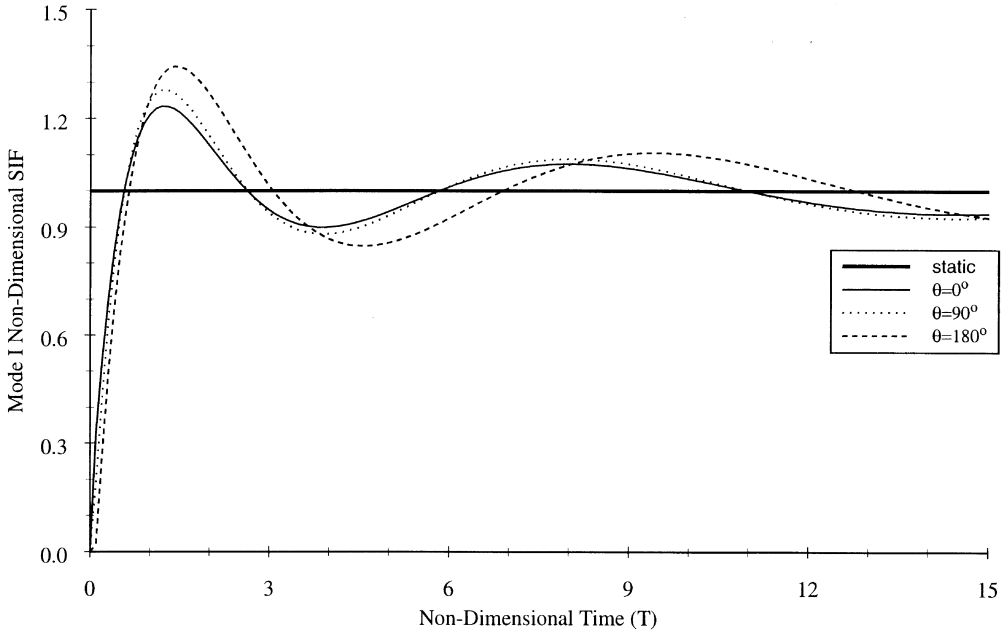

Fig. 7. Non-dimensional SIF for normal applied loads at $\rho_0 = 0.25$, $\alpha = \pm 45.0^\circ$.

that is, as $\rho_0 \to 1$, the contributions from this integral decrease. Therefore, the dynamic stress intensity factor approaches the static value and the amount of dynamic overshoot decreases.

Moving the load from $\rho_0 = 0.25$, $\alpha = 0^\circ$ to $\rho_0 = 0.25$, $\alpha = \pm 45^\circ$ reduced or increased the magnitude of the overshoot depending on whether the load is moved closer or away from the point of interest. As shown in Fig. 7, the magnitude of the overshoot increased at $\theta = 180^\circ$ as the loads were moved from $\alpha = 0^\circ$ to $\alpha = \pm 45^\circ$ because the angular position increased. Note that the time required to reach the overshoot increased. Again, this is because the angular distance between the load position and point of interest increased.

Example 3: *Concentrated radial shear forces*

As an example of the skew-symmetric loading of the crack, we consider a penny shaped crack loaded at $t = 0$ by two radial shear loads of magnitude Q placed at $r = r_0$; $\theta = \pm\alpha$ as shown in Fig. 8.

For the loading under consideration, the radial shear stress may be written as

$$\tau_{rz}(t) = -\frac{Q}{r}\delta(r-r_0)\delta(\theta \pm \alpha) \tag{71}$$

Substitution of (71) into the expressions for the Fourier coefficients (28) leads to

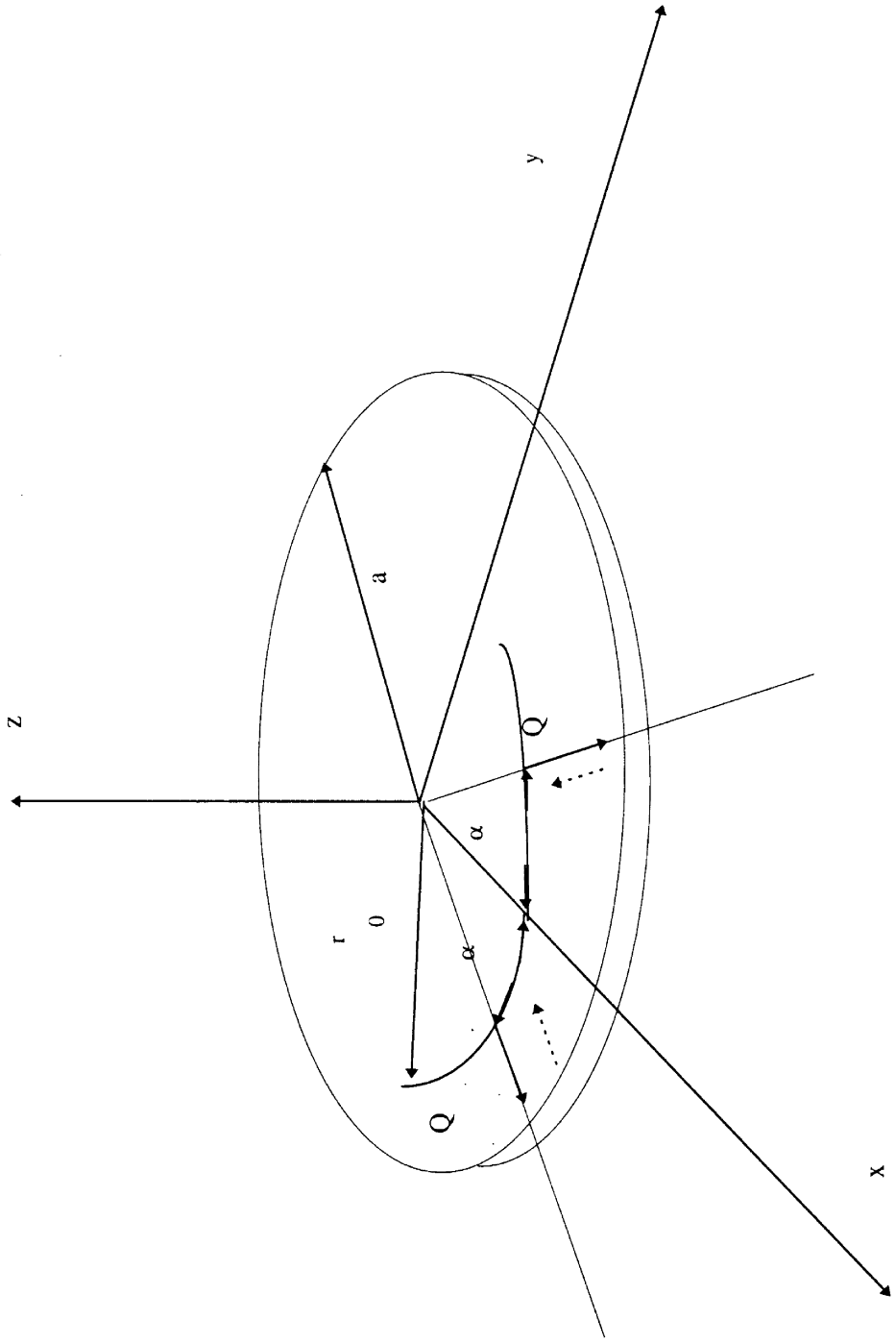

Fig. 8. Penny shaped crack loaded by discrete radial loads Q.

$$c_0 = -\frac{Q}{\pi}\delta(r-r_0)\cos v\alpha \tag{72a}$$

$$c_v = -\frac{2Q}{\pi}\delta(r-r_0)\cos v\alpha \quad v \geqslant 1 \tag{72b}$$

$$d_v = 0 \quad v \geqslant 0 \tag{72c}$$

Then, we may take

$$g(\tau, P) = -\frac{2Qr_0^v\sqrt{\tau}}{\pi(1+N^*)G^*}G(\tau, P)H(\tau-\rho_0)\cos v\alpha \tag{73a}$$

$$\phi_i^v(\tau, P) = -\sqrt{\frac{2}{\pi}}\frac{2Qr_0^v\sqrt{\tau}}{\pi(1+N^*)}F_1^v(\tau, P)H(\tau-\rho_0)\cos v\alpha \tag{73b}$$

Substituting (73a) into (37), we obtain for $v = 0$

$$G(\tau, P)+\frac{2}{\pi}\int_{\rho_0}^{1}\tau s G(s, P)K_2(s, \tau)\,\mathrm{d}s = \frac{1}{\tau^2\sqrt{1-\left(\frac{\rho_0}{\tau}\right)^2}} \tag{74}$$

where

$$K_2(s, \tau) = \int_0^\infty x^2\left[\alpha_1\alpha_2\frac{C_{44}G(ax)}{a_2G^*}-1\right]j_1(x\tau)j_1(xs)\,\mathrm{d}x \tag{75}$$

Substituting (73b) into (44a), we find for $v \geqslant 1$ that

$$F_1^v(\tau)+\frac{2}{\pi}\int_{\rho_0}^{1}\tau s(K_{11}(s, \tau)F_1^v(s)+K_{21}(s, \tau)F_2^v(s))\,\mathrm{d}s = \frac{1}{\tau^v\sqrt{1-\left(\frac{\rho_0}{\tau}\right)^2}} \tag{76}$$

where

$$K_{11}(s, \tau) = \frac{1}{(1+N^*)}\int_0^\infty x^2(g_{11}(ax)+N^*g_{12}(ax))j_{v-1}(xs)j_{v-1}(x\tau)\,\mathrm{d}x \tag{77a}$$

$$K_{12}(s, \tau) = \frac{1}{(1+N^*)}\int_0^\infty x^2(g_{11}(ax)-g_{12}(ax))j_{v+1}(xs)j_{v-1}(x\tau)\,\mathrm{d}x \tag{77b}$$

In equation set (77), $g_{21}(\xi)$ has been replaced by $g_{11}(\xi)$, and $g_{22}(\xi)$ has been replaced by $g_{12}(\xi)$ through expressions (41a) and (41b), respectively.

Likewise, eqn (44b) becomes

$$F_2^v(\tau)+\frac{2}{\pi}\int_{\rho_0}^{1}\tau s(K_{21}(s,\tau)F_1^v(s)+K_{22}(s,\tau)F_2^v(s))\,\mathrm{d}s$$

$$=(1-N^*)\left\{\frac{1}{2\tau^v\sqrt{1-\left(\frac{\rho_0}{\tau}\right)^2}}-\left(v+\frac{1}{2}\right)\sqrt{1-\left(\frac{\rho_0}{\tau}\right)^2}\right\}-(1+N^*)\frac{\rho_0^2}{2\tau^{v+2}\sqrt{1-\left(\frac{\rho_0}{\tau}\right)^2}} \quad (78)$$

with the corresponding kernels (for $v \geqslant 1$)

$$K_{21}(s,\tau)=\frac{1}{2}\int_0^\infty x^2(g_{11}(ax)-N^*g_{12}(ax))j_{v-1}(sx)j_{v+1}(x\tau)\,\mathrm{d}x$$

$$-\left(v+\frac{1}{2}\right)\frac{(1-N^*)}{(1+N^*)\tau}\int_0^\infty x(g_{11}(ax)+N^*g_{12}(ax))j_{v-1}(sx)j_v(x\tau)\,\mathrm{d}x+\frac{(1-N^*)}{2}K_{11}(s,\tau) \quad (79a)$$

$$K_{22}(\zeta,t)=\frac{1}{2}\int_0^\infty x^2(g_{11}(ax)+g_{12}(ax))j_{v+1}(sx)j_{v+1}(x\tau)\,\mathrm{d}x$$

$$-\left(v+\frac{1}{2}\right)\frac{(1-N^*)}{(1+N^*)\tau}\int_0^\infty x(g_{11}(ax)-g_{12}(ax))j_{v+1}(sx)j_v(x\tau)\,\mathrm{d}x+\frac{(1-N^*)}{2}K_{12}(s,\tau) \quad (79b)$$

Again, the stress intensity factors K_{II} and K_{III} may be non-dimensionalized by dividing by the corresponding static values K_{IIS} and K_{IIIS}.

The non-dimensional stress intensity factors become

$$\frac{K_{\mathrm{II}}(T)}{K_{\mathrm{IIS}}}=\frac{1}{2\pi i}\int_{Br}\left[\frac{(1+N^*)G(1,P)+2\sum_{v=1}^{\infty}[\phi_1^v(1,P)-\phi_2^v(1,P)]\rho_0^v\cos v\theta\cos v\alpha}{(1+N^*)G(1,0)+2\sum_{v=1}^{\infty}[\phi_1^v(1,0)-\phi_2^v(1,0)]\rho_0^v\cos v\theta\cos v\alpha}\right]\frac{e(PT)\,\mathrm{d}P}{P} \quad (80a)$$

$$\frac{K_{\mathrm{III}}(T)}{K_{\mathrm{IIIS}}}=\frac{1}{2\pi i}\int_{Br}\left[\frac{\sum_{v=1}^{\infty}[N^*\phi_1^v(1,P)+\phi_2^v(1,P)]\rho_0^v\sin v\theta\cos v\alpha}{\sum_{v=1}^{\infty}[N^*\phi_1^v(1,0)+\phi_2^v(1,0)]\rho_0^v\sin v\theta\cos v\alpha}\right]\frac{\exp(PT)\,\mathrm{d}P}{P} \quad (80b)$$

Again, the inversion required by equation set (80) was carried out by the numerical method of Papoulis (Miller and Guy, 1966). The method of Nystrom (Press et al., 1985) was used to solve the coupled simultaneous integral equations given by eqns (76) and (78).

Even though the external loads are such that there is no torsional load acting on the crack, there

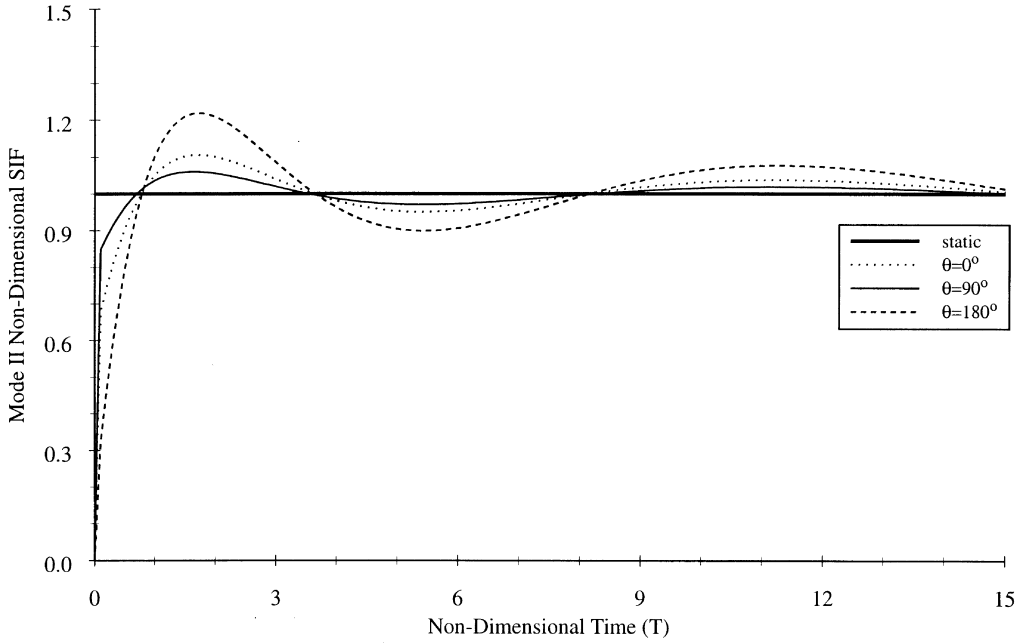

Fig. 9. Mode II non-dimensional SIF for radial shear loading.

is still a mode III stress intensity factor which varies with angular position on the crack. This can be seen from eqn (80b). In the special case of $\theta = 0^\circ$, $K_{III} = 0$.

In Fig. 9, we have plotted the non-dimensional mode II stress intensity factor for $\rho_0 = 0.25$, $\alpha = 0^\circ$. As can be seen from the figure, the SIF varies with angular position. Furthermore, the amount of dynamic overshoot depends on the angular position. For instance, for $\theta = 0^\circ$, the overshoot is 1.15 times the static value and occurs at $T = 1.4$, while at $\theta = 90^\circ$ and $T = 1.6$, the dynamic SIF is 1.06 times the static value. A similar behavior can be seen in Fig. 10, for K_{III}, although $K_{III} = 0$ for $\theta = 0^\circ$, for $\theta = 45^\circ$, the dynamic stress intensity factor reaches a value of 1.077 greater than the static value at $T = 1.8$. When $\theta = 90^\circ$, the corresponding dynamic overshoot is 1.287 times the static value and occurs at $T = 2$.

8. Summary

We have derived the expressions for the non-axisymmetric dynamic loading of a penny shaped crack in a transversely isotropic material. The loading was divided into two parts: the symmetric and skew-symmetric part. Relations for the stress intensity factors were written in terms of Fredholm second type integral equations (symmetric part) and coupled simultaneous Fredholm integral equations (skew-symmetric part). In order to illustrate the solution of these integral equations, as well as to provide solutions which may be used as Green's functions for more complex loadings, two separate numerical examples were considered. The first of these examples involved

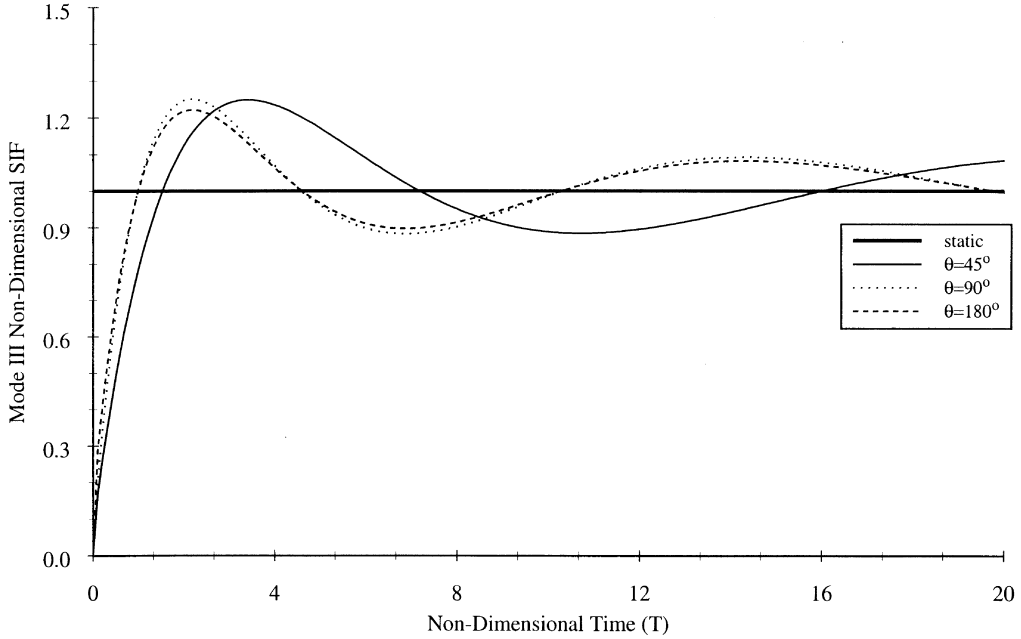

Fig. 10. Mode III non-dimensional SIF due to applied radial shear.

the application of point forces at discrete locations along the crack surface. The second example considered the loading of the crack by discrete radial shear forces.

As typical for impact type dynamic loading problems, the stress intensity factors were found to reach values greater than their static counterparts. This dynamic overshoot varied as a function of angular position on the crack, as well as the exact positioning of the external forces.

In the second example, even though the external loads are such that there is no torsional load acting on the crack, the asymmetry of the loading gives a mode III stress intensity factor as well as a mode II SIF which varies with angular position on the crack.

Acknowledgements

One of the authors (R.R.) would like to thank the Office of Academic Affairs of North Dakota State University for their generous financial research support.

References

Andrews, L. C. (1985) *Special Functions for Engineers and Applied Mathematicians*. Macmillian, New York.

Andrews, L. C. and Shivamoggi, B. K. (1988) *Integral Transforms for Engineers and Applied Mathematicians*. Macmilian, New York.

Chen, W. T. (1966) On some problems in transversely isotropic elastic materials. *Journal of Applied Mechanics* **33,** 317–355.

Chen, B., Gross, D. and Zhang, C. (1996) Axisymmetric dynamic response of a penny shaped crack to a pair of transient concentrated forces. *International Journal of Fracture* **81,** 77–88.

Chen, W. T. and Soni, R. P. (1964) On a circular crack in a transversely isotropic material with prescribed shear stress. *IBM Journal of Research Development* **8,** 192–195.

Christensen, R. M. (1979) *Mechanics of Composite Materials*. Wiley, New York.

Embley, G. T. and Sih, G. C. (1971) Response of a penny shaped crack to impact waves. *Proceedings of the* 12*th Midwestern Mechanics Conference* **6,** 473–487.

Freund, L. B. (1985) *Dynamic Fracture Mechanics*. Cambridge University Press, London.

Kassir, M. K. and Sih, G. C. (1975) *Mechanics of Fracture Volume* 2: *Three-Dimensional Crack Problems*. Noordhoff, The Netherlands.

Krenk, S. and Schmidt, H. (1982) Elastic wave scattering by a circular crack. *Phil. Trans. R. Soc. Lond.* **A308,** 167–198.

Mal, A. K. (1968) Dynamic stress intensity factor for an axisymmetric loading of the penny shaped crack. *International Journal of Engineering Sciences* **6,** 623–629.

Martin, P. A. and Wickham, G. R. (1983) Diffraction of elastic waves by a penny shaped crack: analytical and numerical results. *Proceedings of the Royal Society of London* **A390,** 91–129.

Miller, M. and Guy, W. T. (1966) Numerical inversion of the Laplace transform by the use of Jacobi polynomials. *SIAM J. Numer. Anal.* **3,** 625–635.

Parton, V. Z. and Boriskovsky, V. G. (1989) *Dynamic Fracture Mechanics Volume I Stationary Cracks*. Hemisphere, New York.

Piessens, R. E., deDoncker-kapenga, E., Uberhuber, C. W. and Kahaner, D. K. (1983) *QUADPACK*. Springer-Verlag, New York.

Press, W. H., Teukolsky, S. A., Vetterling, W. T. and Flannery, B. P. (1985) *Numerical Recipes in FORTRAN*. Cambridge University Press, London.

Robertson, I. A. (1967) Diffraction of a plane longitudinal wave by a penny shaped crack. *Cambridge Phil. Society* **63,** 229–238.

Rizza, R. (1995) Dynamic penny shaped crack problems in transversely isotropic materials. Ph.D. dissertation, Illinois Institute of Technology, Chicago, Illinois.

Shindo, Y. M. and Nozaki, H. (1987) Impact response of a transversely isotropic cylinder with a penny shaped crack. *International Journal of Solids and Structures* **23,** 187–199.

Sih, G. C. (1977) *Mechanics of Fracture Volume* 4: *Elastodynamic Crack Problems*. Noordhoff, The Netherlands.

Sih, G. C. and Chen, E. P. (1981) *Mechanics of Fracture Volume* 6: *Cracks in Composites Materials*. Martinus Nijhoff, The Netherlands.

Sih, G. C. and Embley, G. T. (1972) Sudden twisting of a penny shaped crack. *Journal of Applied Mechanics* **39,** 395–400.

Sih, G. C. and Loeber, J. F. (1969) Normal compression and radial shear waves scattering at a penny shaped crack in an elastic solid. *Journal of the Acoustical Society of America* **46,** 711–721.

Sneddon, I. N. (1966) *Mixed Boundary Value Problems in Potential Theory*. North-Holland, The Netherlands.

Sokolnikoff, I. S. (1987) *Mathematical Theory of Elasticity*. Krieger, Malabar, Florida.

Tsai, Y. M. (1988) Dynamic penny shaped crack in a transversely isotropic material. *Engineering Fracture Mechanics* **31,** 977–984.

Westmann, R. A. (1965) Simultaneous pairs of dual integral equations. *SIAM Review* **7,** 341–348.